Flow regime effects on the spreading rate of a nylon fiber suspension jet in a rectangular channel

ERIC ANDREW SCHMIDT AND JUNYONG ZHU

ABSTRACT: A fiber suspension jet was symmetrically introduced to a dilution water flow in a rectangular Plexiglas test section. The fiber suspension was disrupted by a flow restriction located in the nozzle prior to the mixing region. Digital imaging was used to observe the behavior and growth of the mixing layer, which was correlated to the pressure drop across the restriction. The growth of the shear layer was affected primarily by the difference in velocity between the fiber suspension flow and the dilution water flow, when the fiber suspension jet was highly turbulent. Finally, the mixing layer became less uniform with an increase in fiber length and suspension concentration and with a decrease in the pressure drop across the flow restriction.

Application: Concentration, fiber length, and flow parameters affect the behavior of fiber suspensions in a confined shear flow.

Papermakers dilute thick stock in the approach flow to a paper machine by creating shear between a stream of dilution water and a concentrated jet of pulp. Dilution reduces the mass concentration of the fibers in the suspension to reduce nonuniformities in the suspension and produce a more uniform sheet of paper.

In this research on the shear dilution of a fiber suspension, we use high-speed digital imaging to measure the effects of various parameters on mixing in a laboratory apparatus. In research already presented [1], we focused on developing a quantitative relationship between the stream velocities and the rate of mixing, as indicated by the boundary angle between the two streams. In this phase of the work, our objective was to separate the velocity ratio effect from the shear effect. To separate these effects on the mixing efficiency, we changed the pressure drop across a flow restriction in the nozzle and observed the effects on the growth of the shear layer and on the quality of the mixing field.

BACKGROUND

The characterization of the fiber suspension dilution process has been primarily qualitative or based on largely averaged measurements. Still, some idea of the primary factors affecting this process can be gained from previous work. For example, Norman and Tegengren determined by qualitative, visual observation that the velocity difference between the fiber suspension and dilution water streams is a primary factor [2]. The ideal velocity difference was determined when the jet behaved more like a turbulent jet in the mixing region.

Covey *et al.* used a sampling probe downstream of the jet exit to obtain radial fiber concentration distributions for suspensions of short fibers (virgin bleached eucalypt kraft) and long fibers (virgin bleached softwood kraft) [3]. Although the probe was intrusive in the flow and measurements were significantly averaged in time and space, this study added important information on the spreading rate of the jet.

Mixing in confined flows is a process that occurs on several scales. In the dilution of thick stock approaching a paper machine, efficient and uniform distribution on the macro- and meso-scales is the primary objective. Macro-scale mixing is mixing arising from flow instabilities on the scale of the pipe length. Meso-scale mixing is mixing of the flocks resulting from turbulent convection.

The mixing mechanisms for thick stock dilution can be described from confined jet flows. For a confined turbulent jet, as illustrated in **Fig. 1**, the entrainment rate of the secondary fluid is simply a function of the jet boundary angle α [4]. Therefore, the angle defined by the turbulent jet boundary is also the rate at which the jet spreads and is a good indication of the efficiency of macro-scale mixing.

The primary macro-scale mixing mechanism in shear flows is the Kelvin–Helmholtz instability [5], which results from differences in velocities between the primary and secondary streams. The scaling factor, λ, is used to compare spreading rates in shear flows [6–12] and is shown in Eq. 1. This factor corrects the growth in the shear layer to the combined rate of downstream convection.

$$\lambda = (U_1 - U_2)/(U_1 + U_2) \qquad (1)$$

where
U_1 = fiber suspension stream (higher velocity)
U_2 = dilution stream (lower velocity).

The meso-scale mixing mechanism of turbulent convection is significantly affected by the presence of fibers in a fiber suspension flow field. Bugliarello and Daily found that the addition of fibers increases the rate of turbulence decay in a given flow field [13], and Walseth arrived at similar conclusions [14]. This dampening of the turbulence field has a negative impact on the convective transport of mass and momentum and has been directly observed for fiber-laden liquid jets [15].

The initial conditions of the jet, prior to the shear field, may also influence mixing. For example, Mi *et al.* observed that the spreading of gas flows depends on the initial conditions of the jets [16]. Likewise, fiber suspension jet flows could exist as one of several flow regimes defined by the relative turbulence activity in the suspension [17–20]. Generally, the flow regime is a function of the fiber length and flexibility, the suspension concentration, the pipe size, and the pipe

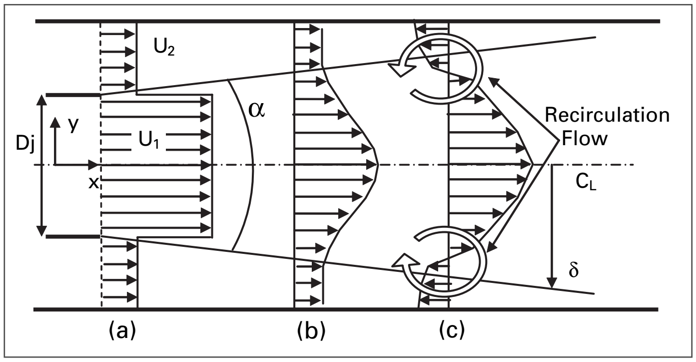

1. Confined coaxial jet flow showing recirculation.

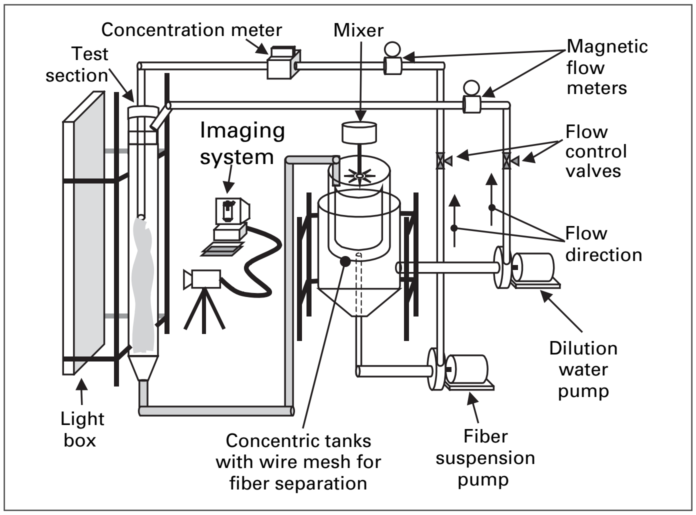

2. Flow loop schematic.

surface roughness, and the flow becomes more turbulent as the flow velocity increases [21–25]. Furthermore, the suspension properties affecting the flow regime are related to the suspension yield stress. Bennington *et al.* found that nylon fiber suspensions have a yield stress in the following form [24], with coefficient values of $a = 84.4$, $b = 2.5$, and $n = 1$:

$$\tau_y = aC^bA^n \tag{2}$$

where

τ_y = suspension yield stress, Pa

C = volumetric concentration fraction of fibers, mL/mL

A = fiber aspect ratio.

Disruption of the fiber network, or fluidization of the suspension, has been shown to improve mixing within a fiber suspension. For example, Francis and Kerekes correlated the degree of mixing of Astra Red P liquid dye in a fiber suspension to the pressure drop across a valve in a 10 cm pipe [26]. They found that the networks of fiber suspensions up to 13%–14% concentration could be completely disrupted and that such a disrupted suspension behaved much like turbulent water for pressure drops greater than 200 kPa.

Both Norman and Tegengren [2] and Covey *et al.* [3] suggest that the velocity ratio between the jet and the co-flow should be at least 7:10 to achieve good mixing. This velocity ratio is well above the TAPPI minimum recommendation of 1.1 [27]. However, in both studies, the fiber jet velocity was increased to increase the velocity ratio. This adjustment also increased the shear acting on the suspension in the nozzle. To determine the true effect of the velocity ratio, the shear should be decoupled from the flow regime.

The main objective of our research was to decouple the velocity ratio effect from the shear effect on the mixing efficiency of a thick stock dilution process. To separate these effects, we changed the pressure drop across a flow restriction in the nozzle at equivalent velocity differences and observed the effect on the growth of the shear layer and the quality of the instantaneous mixing field.

EXPERIMENTAL

We used nylon fiber in this work because natural fibers degrade and are not uniform in length. We used two different lengths of nylon fiber, 0.635 mm and 1.27 mm. The fibers of both lengths were 14.9 µm in diameter, resulting in aspect ratios of 42.6 and 85.2, respectively. The yield stress for each suspension was calculated from Eq. 2.

Apparatus

The fiber suspension and dilution flows were pumped via separate centrifugal pumps from the main tank, as shown in **Fig. 2**, and flow rates were measured by magnetic flowmeters. To allow for continuous operation, we designed a fiber filtering system to separate fibers from the dilution water. The filtering system consisted of concentrically arranged plastic tanks. Large rectangular holes were cut out of the smaller concentric tank and were sealed with a fine wire mesh of stainless steel. The mixed flow from the test section was returned to the central small tank, where an axial-blade, industrial agitator continuously stirred the return suspension to keep it well mixed.

An optical concentration meter was located on the fiber suspension piping to confirm the fiber suspension concentration entering the mixing channel. This meter was developed specifically for this research and was based on well-proven methods of measuring optical concentration [28–30]. The meter measured transmitted light intensity with a photodetector and was well correlated ($r^2 > 0.98$) to the concentration of the flowing suspension [31].

The symmetric mixing channel was 22.9 cm wide by 1.27 cm deep, and the length of the mixing section was 1.9 m. A divider separating the dilution and fiber streams extended 0.5 m into the mixing channel to allow the flows of the dilution water and fiber suspension to develop. The divider was placed in the middle of the channel, so that the jet width was 2.54 cm. The dilution water channels were 10.16 cm wide on each side of the nozzle dividers. The nozzle dividers were made of 1 mm thick copper plating to minimize wake effects from the tips.

A removable nozzle insert, or flow restriction, was located 10 cm from the nozzle exit in the symmetric rectangular test channel. The nozzle insert was added to increase the pressure drop in the nozzle by reducing the flow area from 323 mm² to 194 mm². The area was reduced symmetrically on either side of the nozzle centerline with 5 mm round pegs, which reduced the width of the nozzle from 25.4 mm to 15.4 mm. The depth of the nozzle was unchanged by the nozzle insert and remained at 12.7 mm.

Pressure taps were located in the nozzle 10 cm apart. The pressure taps were 5 cm upstream and 5 cm downstream of the nozzle insert, as shown in **Fig. 3**. The pressure was measured by

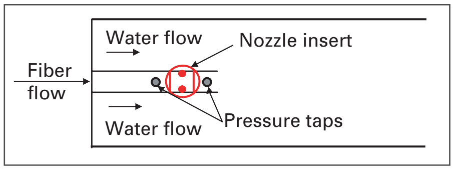

3. Test channel.

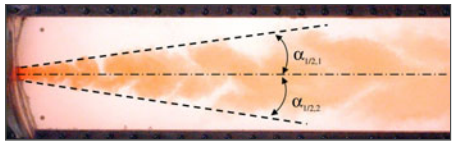

4. Dye tracer image at a velocity ratio of R_v = 6 in the symmetric test section.

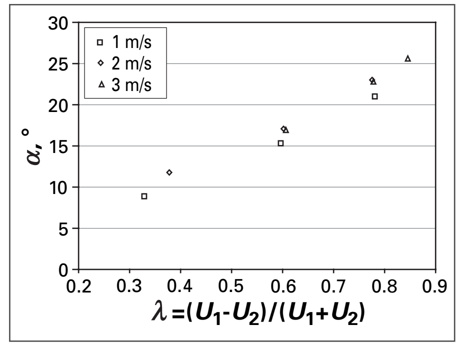

5. Dye tracer boundary angle in symmetric test section.

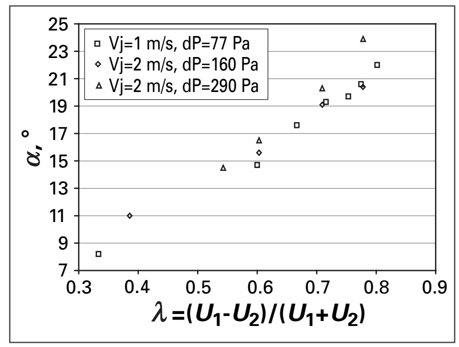

6. Pressure drop effect on 0.635 mm fiber at 1% suspension concentration with the nozzle insert.

a 5-psi differential pressure transducer.

A digital camera (Canon ES310) and PCI capture board were used to image the flow in the channel. The digital camera was placed on the opposite side of a high-intensity, diffuse light source. The mixing channel was located between the camera and the light source. The camera resolution was 640 by 480 pixels.

Procedure

We determined the boundary angle between the wake boundaries and the line extending from the nozzle tip parallel to the flow direction. The half angle of the jet near field ($x \leq 12 - D_j$) was determined above and below the jet centerline and was added to obtain the full angle. We used an image analysis routine to make the boundary angle measurement, as described in detail elsewhere [31].

Briefly, the measurement was made from an averaged image of 30 images that spanned a time greater than 10 times the flow residence time for each set of experimental conditions. The measurement was repeated three times for each condition, for a total of 90 images. The measured angles were averaged at each condition, yielding standard deviations typically between 0.038 and 0.4. The standard deviation was not correlated to suspension concentration, fiber length, flow velocity, or measurement magnitude.

Three jet volumetric flow rates were used for the fiber suspension, corresponding to mean velocities of 1 m/s, 2 m/s, and 3 m/s. The Reynolds numbers for equivalent water flows were 9.45×10^3, 1.92×10^4, and 2.84×10^4, respectively. The pressure drops across the nozzle insert at these flow rates were approximately 2.8 kPa, 6.9 kPa, and 11 kPa, respectively, and corresponded to effective wall stress values of approximately 75 Pa, 180 Pa, and 300 Pa. Without the nozzle insert, the pressure drops at these flow rates were approximately 0.21 kPa, 0.55 kPa, and 0.97 kPa, respectively, corresponding to calculated wall stresses of approximately 5 Pa, 13 Pa, and 26 Pa.

The flow velocities for the dilution water were between 0.1 m/s and 0.9 m/s and depended on the ratio of the desired velocity to the fiber suspension. These velocities corresponded to a Reynolds number between about 1.58×10^3 and 1.14×10^4. Hence, both streams were considered turbulent for equivalent water flows. No plug flow behavior was observed at any condition when the nozzle insert was in place. However, some plug flow behavior was observed when the nozzle insert was removed at suspension concentrations over 4% by mass for both fiber lengths. In addition, at these concentrations, the suspension was prone to plug between the planes orthogonal to the camera view downstream of the jet exit.

Concentrations for the 0.635 mm fiber length were 1% and 10% by mass. For these concentration levels, boundary angles are reported with the nozzle flow restriction in place. For the suspension with 1.27 mm fibers, the boundary angle was observed at 5% concentration with and without the nozzle flow restriction.

RESULTS

The central thesis of this work is that disruption of the fiber network prior to the mixing region will improve the mixing performance of a fiber dilution process. Both quantitative (spreading rate) and qualitative (instantaneous images) are presented as evidence.

Dye tracer benchmarking

Figure 4 illustrates the mechanism for the spread of the mixing region for the case of water and dye mixing without the flow restriction in the nozzle. Instability in the mixing region grows with axial distance from the jet exit into large-scale vorticies, which engulf and fold the secondary stream into the mixing region.

As shown in **Fig. 5**, the most significant factor for the growth of the water–dye boundary layer in this system is the velocity difference, or λ. Linear trends fit to each case show the slopes to be 26.6°/λ, 28°/λ, and 35.9°/λ for jet velocities of 1, 2, and 3 m/s, respectively. Overall, the slopes average 30.2°/λ. When the boundary angles are compared at a given λ, only a slight difference is evident between the 1 m/s case and the cases for the other two jet velocities. The slight increase in the boundary angle from the 1 m/s case is caused by the increased turbulence intensity in the jet and the increased velocity difference between the two streams ($U_1 - U_2$). However, the angle at a given λ asymptotically approaches a maximum above 1 m/s, and further increases in the jet velocity do not affect the boundary angle. This phenomenon is evident from the 2 m/s and 3 m/s jet velocity data presented in Fig. 5.

The boundary angle increase over the range of λ illustrates the significance of the velocity difference ($U_1 - U_2$) on the spreading rate of the jet. For example, increasing the jet velocity above 1 m/s at a fixed λ increased the boundary angle by only 1.73°. By comparison, increasing the velocity difference at a fixed jet velocity increased the boundary angle approximately 5° over the range of λ.

Short fiber suspension behavior

Adding short fibers to the jet stream and inserting the nozzle flow restriction had a small effect on the boundary angle when the suspension concentration was low. For example, the boundary angle

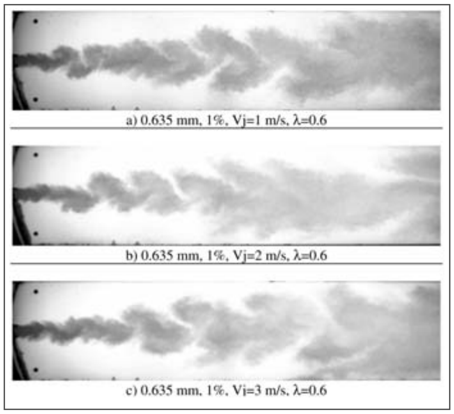

7. Instantaneous images of 0.635 mm fiber at 1% suspension concentration with the nozzle insert.

results for the suspension of 0.635-mm fibers at 1% concentration are shown in **Fig. 6**. The overall average of the linear trend slopes for these data sets is 30.9°/λ, which is about the same as the average slope for the data on water and dye mixing.

The boundary angle increase caused by the increased jet velocity at a given λ is also similar to the case of water–dye mixing. The difference between the low jet velocity of 1 m/s (*dP* = 77 Pa) and the high jet velocity of 3 m/s (*dP* = 290 Pa) is approximately 1.70° over the range of velocity differences, λ, and is about the same as the water–dye case without the flow restriction. For the medium jet velocity of 2 m/s (*dP* = 160 Pa), boundary angles appear to fall between the low and high angles of jet velocity.

Figure 7 presents the corresponding instantaneous images for the suspension of 0.635 mm fibers at 1% concentration. The large-scale eddy mechanism grows the shear layer in an odd instability mode and is similar to the mechanism for water–dye mixing. The images are compared at λ = 0.6 for all three jet velocity cases. For λ below 0.6, the experimental conditions were not exactly comparable at this suspension case. Above λ of 0.6, the mixing phenomena were similar to the phenomena captured in the images in Fig. 7.

As the instantaneous images show, the instability begins between 2 and 3 jet widths downstream from the jet exit in all three cases. The instability continues to grow downstream in an odd mode, and the resulting eddies tend to pair after about 10 jet widths downstream. For the case of the 1 m/s jet velocity, compared to the other two cases, the eddy pairs

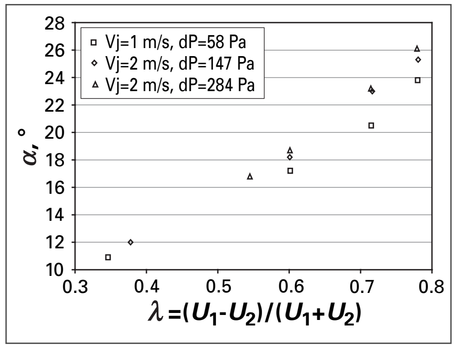

8. Pressure drop effect on 0.635 mm fiber at 10% suspension concentration with the nozzle insert.

appear to maintain a more coherent structure far downstream of the jet exit. This difference may explain why the boundary angle is less for the 1 m/s case. The difference is likely caused by the lower intensity of the turbulence in the case of the 1 m/s jet. This trend was also observed in the water–dye mixing and could also be due in part to the lower actual velocity difference ($U_1 - U_2$) in the case of the 1 m/s jet.

Also, the frictional forces are not likely to be dampening the shear layer growth at the upper and lower boundaries (parallel to the image plane) of the channel depth. Fiber suspensions have less drag than water or exhibit drag behavior similar to that of water in the transition and turbulent flow regimes. Inertial effects are dominant in all the jet velocity cases. The flow regime of the fiber suspension was observed to be highly turbulent just after the jet exit, and it appeared turbulent far downstream in the mixing region as well. This observation correlated well with the ratio of predicted suspension yield stress to the pressure drop across the flow restriction, which was less than 0.18 Pa to 75 Pa for all three jet velocities. It also correlated well with the ratio of predicted suspension yield stress to the minimum calculated wall stress in the mixing region, which was less than 0.18 Pa to 0.34 Pa for all three jet velocities.

Suspension concentration effect on flow behavior

By increasing the fiber suspension concentration an order of magnitude, we observed the concentration effects on the boundary angle. **Figure 8** shows the pressure drop effects at a fiber concentration of 10%. The overall average of the linear trend slopes for these data sets is 32.8°/λ, which again is about the same as

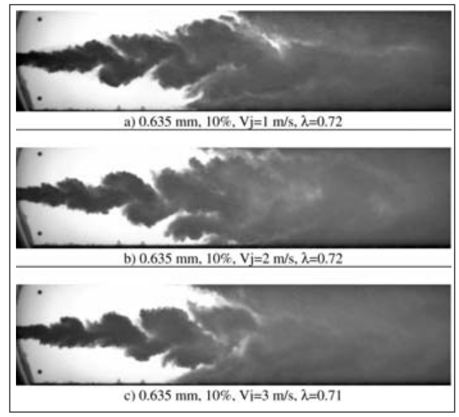

9. Instantaneous images of 0.635 mm fiber at 10% suspension concentration with the nozzle insert.

the water–dye mixing and 1% mixing data. However, the slightly higher average slope for this condition is caused by some systemic error in the measurement method, resulting from the very high suspension concentration for this case.

While the results are comparable within this case, the exact boundary angle values are not necessarily comparable to cases with lower suspension concentrations. Still, the boundary angle increase from the case of the 1 m/s jet velocity is an average of 2.2° over the range of λ. In comparison, both the 2 m/s and 3 m/s jet velocities have boundary angles within an average of 0.5° over the range of λ. Again, this increase in boundary angle is caused by the increase in the velocity difference and the increase in the jet turbulence intensity, which is significantly increased by the nozzle insert in this case.

For the case in Fig. 8, the suspension flow regime was difficult to judge because the high concentration complicated the visual assessment. However, the suspension jet did appear turbulent, and the mixing layer mechanism appeared qualitatively similar to the 1% concentration case in the near field, as shown for λ ≈ 0.71 in **Fig. 9**. Turbulence in the near field also seems likely since the pressure drop across the flow restriction was always greater than the predicted yield stress of the suspension for this case. In comparison, the ratio of the predicted yield stress to the pressure drop across the flow restriction approached 1 for the 1 m/s jet and indicates that the initial conditions for the jet may not have been fully turbulent. This lack of full turbulence correlates with the depressed boundary angle at this condition.

For the 2 ms and 3 m/s conditions, the pressure drops across the flow restriction were 3 times and 6 times greater than the predicted suspension yield stress, and the jet was probably highly turbulent. Since the boundary angles were much closer for these conditions over the range of λ, this outcome suggests that the spreading rate is fairly constant at a given λ as long as the jet initial condition is highly turbulent and the fiber network is disrupted prior to being introduced to the shear flow.

Behavior of the suspension with long fiber

To better understand the effect of the initial jet conditions on the spreading rate, we obtained boundary angles for the 1.27 mm fiber length at 5% concentration with and without the flow restriction in the nozzle, as shown in **Fig. 10**. Boundary angles for the case without the flow restriction are identified by the data points for the 15 Pa and 23 Pa pressure drops, which correspond to the 2 m/s and 3 m/s jet velocities. These measured values for pressure drop also correlate well with the calculated Blausius wall stress [32]—within ±3 Pa.

At the 1 m/s jet velocity, the suspension flow formed a plug downstream of the jet exit whenever the flow restriction was not in place. This development is expected with the predicted yield stress for the suspension being approximately 27 Pa. The flow regime was also difficult to observe visually for this fiber suspension at the 2 m/s and 3 m/s jet velocities, but it appeared to be plug flow or mixed flow.

The 74 Pa, 170 Pa, and 294 Pa data points in Fig. 10 represent the average pressure drops across the nozzle flow restriction for the jet velocities of 1, 2, and 3 m/s. The flow regime of the suspension appeared turbulent for all three jet velocities with the flow restriction in place. Overall, the boundary angles for these data sets are an average of 4.6° greater than the boundary angles without the flow restriction over the range of λ. This difference is a significant change in the spreading rate of the jet and is a clear indication that the initial jet conditions affect the mixing behavior.

Figure 11 shows the cases with and without nozzle flow restriction for the 5% suspension with 1.27 mm fibers.

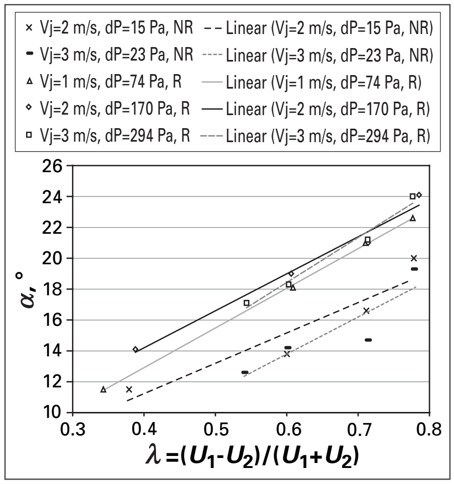

10. Comparison of boundary angles of the 1.27 mm fiber at 5% concentration in the symmetric test section without the nozzle insert.

Image A shows the downstream plugging at the 1 m/s case, and Image B shows the dramatic improvement made in the downstream mixing behavior when the flow restriction is placed in the nozzle. Likewise, Images C and D and Images E and F show similar improvements at the 2 m/s and 3 m/s jet velocities when no downstream plugging of the suspension is evident.

These image pairs also show a decrease in nonuniformity in the mixing region when the flow restriction is in place. The decrease in the shear layer nonuniformity is also caused by the higher intensity of turbulence of the jet in these cases. Decreases in nonuniformity, as caused by the flow restriction, were observed over the entire range of λ for this case (5% concentration of 1.27 mm fibers). These decreases indicate that the overall mixing quality may be improved along with the spreading rate. Finally, since the decrease in structural nonuniformity correlates to an increase in the jet spreading rate, this result supports the hypothesis that disruption of the fiber network prior to mixing will improve the mixing behavior at any given velocity difference.

CONCLUSIONS

The spreading rate is a function of the velocity difference and the flow regime. Increases in the suspension concentration and fiber length decrease the spreading rate of a two-dimensional, confined suspension jet in a dilution co-flow by changing the jet flow regime. When

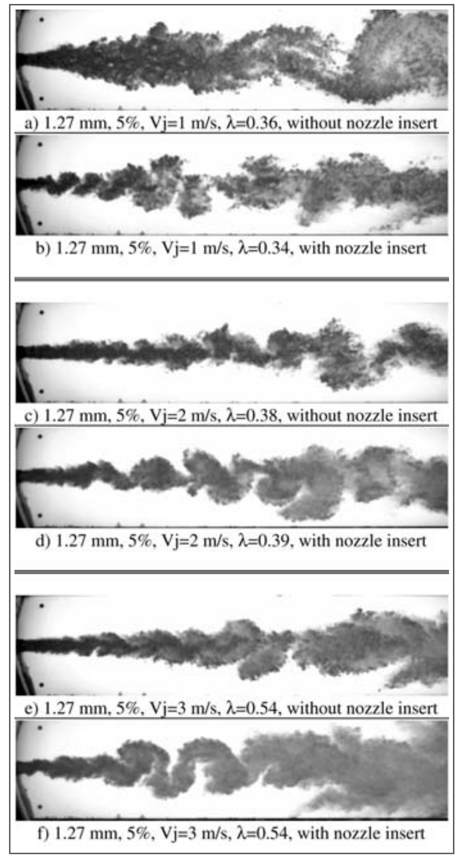

11. Instantaneous images of 1.27 mm fiber at 5% suspension concentration without and with the nozzle insert.

the suspension jet is highly turbulent, the spreading rate depends only on the velocity difference. However, if the flow regime tends towards mixed or plug flow, then the spreading rate decreases for a given difference in velocity.

Finally, the spreading rate and degree of nonuniformity in the mixing region is significantly improved when a flow restriction is placed in the jet nozzle just upstream of the nozzle exit. For a flow geometry on the scale used in this experiment, the spreading rate and the degree of nonuniformity improve when the pressure drop across the flow restriction is at least 2 or 3 times greater than the predicted yield stress of the nylon fiber suspension. **TJ**

LITERATURE CITED

1. Schmidt, E.A., and Zhu, J., *TAPPI J.* 3(11): 11(2004).
2. Norman, B., and Tegengren, A., *Paper Technol.* 31(1): 42(1990).
3. Covey, G.H., Helmer, R.J.N., and Lai, L.C.-Y., *Appita J.* 52(3): 197(1999).
4. Gibson, M.M., "Hydrodynamics of confined coaxial jets,"

Encyclopedia of Fluid Mechanics (N.P. Cheremisinoff, Ed.), Vol. 1, Gulf Publishing Co., Houston, 1986.
5. Browand, F.K., and Winant, C.D., *J. Fluid Mech.* 63(2): 237(1974).
6. Brown, G.L., and Roshko, A., *J. Fluid Mech.* 64: 775(1974).
7. Miles, J.B., and Shih, J., *AIAA J.* 6: 1429(1968).
8. Mills, R.D., *J. Fluid Mech.* 33: 591(1968).
9. Pui, N.K., “The plane mixing layer between parallel streams,” M.S. thesis, University of British Columbia, 1969.
10. Spencer, B.W., and Jones, B.G., *American Institute of Aeronautics and Astronautics Journal* 71: 613(1971).
11. Yule, A.J., *Aero. Res. R. & M.* 3683(1972).
12. Slessor, M.D., Zhuang, M., and Dimotakis, P.E., *J. Fluid Mech.* 414: 35(2000).
13. Bugliarello, G., and Daily, J.W., “The effects of fibers on velocity distribution, turbulence, and flow resistance of dilute suspensions,” MIT Technical Report No. 30, Hydrodynamics Laboratory, October 1958.
14. Walseth, D.S., “An investigation of time-mean velocity and consistency distributions in a fiber suspension jet,” Ph.D. thesis, IPC, Appleton, Wis., January 1976.
15. Filipsson, L.G.R., Lagerstedt, J.H.T., and Bark, F.H., *J. Non-Newtonian Fluid Mechanics* 3: 97(1977/1978).
16. Mi, J., Nobes, D.S., and Nathan, G.J., *J. Fluid Mech.* 432: 91(2001).
17. Mason, S.G., and Robertson, A.A., *Tappi* 40(5): 326(1957).
18. Seely, T.L., “Turbulent tube flow of dilute fiber suspensions,” Ph.D. thesis, IPC, Appleton, Wis., January 1968.
19. Gullichsen, J., and Härkönen, E., *Tappi* 64(6): 69(1981).
20. Xu, H., and Aidun, C.K., *TAPPI 2001 Engineering Finishing and Converting Conference,* TAPPI PRESS, Atlanta, p. 13.
21. Thalen, N., and Wahren, D., *Svensk Papperstid.* 67: 474(1964).
22. Duffy, G.G., and Titchenner, A.L., *Svensk Papperstid*. 78(13): 474(1975).
23. Bennington, C.P.J., Grace, J.R., and Kerekes, R.J., *Can. J. Chem. Eng.* 68(5): 748(1990).
24. Bennington, C.P.J., Azevedo, G., John, D.A., *et al.*, *JPPS* 21(4): J111(1995).
25. Bugliarello, G., and Daily, J.W., *Tappi* 44(7): 497(1961).
26. Francis, D.W., and Kerekes, R.J., *Tappi J.* 75(9): 113(1992).
27. *Headbox Approach Piping Guidelines,* TAPPI TIP 0404-54, TAPPI PRESS, Atlanta, 2000.
28. Barron, R.L., Bentley, R.G., and Jack, J.S., *Pulp Paper Can.* 91(2): 59(1990).
29. Lavigne, J.R., *Paper Age* 101(8): 34(1985).
30. Jansson, I., *Accurate Consistency: A Handbook on Consistency Measurement in Pulp and Paper Processing*, Säffle, Sweden, BTG Pulp & Paper Technology AB, 1999.
31. Schmidt, E.A., “Characterization of a fiber suspension jet in a co-flow dilution process,” Ph.D. thesis, IPST, Atlanta, 2003.
32. White, F.M., “Incompressible Turbulent Mean Flow,” in *Viscous Fluid Flow*, 2nd edn., McGraw-Hill, St. Louis, 1991, p. 394.

Received: June 2, 2004
Revised: March 15, 2005
Accepted: March 16, 2005

This paper is also published on TAPPI’s web site <www.tappi.org> and summarized in the June *Solutions! for People, Processes and Paper* magazine (Vol. 88 No. 6).

INSIGHTS FROM THE AUTHORS

Multiphase, non-Newtonian flows involving mixing and dilution are broadly significant in several industries and still largely uninvestigated. Also, pursuing this research fulfilled a natural curiosity for two scientists with a background in fluid mechanics.

Our previous research explored the effect of flow regime on the spreading rate of fiber suspension jets. Because we previously allowed the flow regime to develop naturally as a function of jet velocity, suspension concentration, and fiber length, we could not completely examine the effect of the network on mixing. In this research, we more fully explored the effect by studying disrupted and undisrupted networks at similar flow conditions.

Controlling the initial concentration and flow rate of the fiber suspension were the most difficult aspects of this research. Developing a steady state process and a fiber filtration system also required considerable development time.

From our previous results, we suspected that both the large scale mixing mechanisms and flock-scale non-uniformities would be significantly affected by disrupting the network in the suspension jet. However, the extent of change in flock-scale non-uniformity was surprising.

The significant change in the flock-scale non-uniformity is perhaps most intriguing for application in full-scale, industrial operations and suggests that fairly appreciable gains in mixing efficiency may be gained through simple process modifications.

While doing this research, we received inquires regarding our intent to study natural fiber suspensions. Because the properties of natural fiber suspensions are as varied as the fiber properties from which they are comprised, empirical correlations may need to be developed for each individual furnish and possibly in real time. In order to manage this variability, new and more advanced measurement and control technologies should be developed to take advantage of the concepts presented in this paper.

Schmidt

Zhu

At the time of this research Schmidt was with the Institute of Paper Science and Technology, 500 10th St., NW, Atlanta, GA 30318. He is now with the Swedish Pulp and Paper Research Institute, Box 5604, SE-114 86 Stockholm, Sweden. Zhu is with the USDA Forest Products Laboratory, One Gifford Pinchot Dr., Madison, WI 53705. Email Schmidt at eric.schmidt@easchmidt.com.